Double Wedge Shockwave Interaction Flow Characterization

Syed Shah[1], Ramon Martinez[2], Nelson Fernandez[3], and Nikos J. Mourtos[4]

Aerospace Engineering
San Jose State University
One Washington Square
San Jose, CA, 95192-0087

Phenomena associated with the interaction of shock waves has long been known to present critical challenges in the design of supersonic and hypersonic vehicles. For example, aerodynamic heating and pressure loads may increase greatly when such interactions are present. In this paper we perform Computational Fluid Dynamics (CFD) analysis of these shockwave interaction flows and compare our results with previously published data. More specifically, the objective of our project is to characterize the flow of double wedge shock interactions using CFD analysis. Conditions of types 4, 5, and 6 shock interactions are studied. The geometry used to generate the primary and secondary shocks is that of a 2D axi-symmetric double wedge geometry. We then compare our computations with published data to validate our modeling of these shock interactions. Our analysis successfully characterized type 4, 5, and 6 shock interactions. In general, very similar outflows were seen when compared to results of previously published data, which are used as benchmarks. We were able to generate and capture the shocks generated at the intersection points for the three different types of shock interactions. The downstream flow also experienced the frequently encountered supersonic jet, which extends in most cases, all along the near surface of the wedge and other commonly associated physics with these interactions. Slip lines were also observed in a location similar to the location shown in the benchmark cases.

Nomenclature

L_1	=	Initial surface wedge length
L_2	=	Second surface wedge length
θ_1	=	Angle of first wedge surface with respect to initial horizontal surface
θ_2	=	Angle of second wedge surface with respect to initial horizontal surface
M	=	Free stream Mach number

I. Introduction

THE shock-shock phenomena occurring in supersonic and hypersonic flows present critical challenges in the design of supersonic and hypersonic vehicles. Aerodynamic heating and increased pressure loads are two such challenges as highlighted in the cases of the X-15 and the space shuttle. On the other hand, the shock-shock interactions can be utilized to increase drag and improve the aerodynamic deceleration of these vehicles during reentry.

Previous investigators have used Computational Fluid Dynamics (CFD) to study the flow conditions necessary for differentiating shock interactions. The main focus of their work was the classification and understanding of Edney Type I, II, III, and IV interactions. As seen in the work of Grasso[8], Olejniczak[9], and Edney[4], shock interactions have been of great interest to the aerospace community for many years. Grasso[8] focuses on the various

[1] Student, Department of Aerospace Engineering, One Washington Square, San Jose, CA 95192-0087.
[2] Student, Department of Aerospace Engineering, One Washington Square, San Jose, CA 95192-0087.
[3] Student, Department of Aerospace Engineering, One Washington Square, San Jose, CA 95192-0087.
[4] Professor, Department of Aerospace Engineering, One Washington Square, San Jose, CA 95192-0087.

shock–shock interference patterns that occur, and presents theoretical approaches to: (1) determine and characterize the conditions for the transition from one Type to another, and (2) estimate the aerodynamic and thermal loads for the most critical interactions. He continues with an experimental investigation of Type III and Type IV interactions and assesses the influence of the impinging shock strength on the formation of a supersonic jet on the downstream flow. He concludes that the supersonic jet exhibits a change in shape from perpendicular to curved as the shockwave strength increases. Grassos' analysis also shows that shock interactions may experience a hysteresis phenomenon, which is typical of steady shockwave reflections. Edney[4] and Oljniczak[9] performed experimental and computational investigations of shock interactions. They used CFD to study inviscid shock interactions on double-wedge geometries for the purpose of understanding the fundamental gas dynamics of these interactions. They explored the parameter space of the interaction and identified the different Types of interactions that occur. They studied the physical mechanisms for transition and identified the transition criteria.

II. Modeling Methodology

The software used in the modeling and analysis for this project was ESI-Suite. This standalone software package that comes with ESI-Suite and was used for this project includes:

1) CFD-GEOM: a CAD and meshing software package.
2) CFD-FASTRAN: a supersonic structured and unstructured CFD solver.
3) CFD-VIEW: a postprocessor and analysis package.

III. Approach

Figure 1 shows a schematic of the 2-D axisymmetric geometry for a double wedge. There are six distinct flow structures that have been classified as Type I through Type VI shock-shock interactions. In our study we modeled Type IV, V, and VI shock-shock interactions for the same given inflow conditions. The Type of shock-shock interaction generated depends solely on the outflow geometry and freestream Mach number. Figure 1 shows that the flow conditions generated for the double wedge geometry depend on the four geometric parameters L_1 and L_2 (the length of the first and second wedge deflection surfaces) and θ_1 and θ_2 (the flow deflection angles measured from the freestream direction). Hence, it is possible to generate different shock interaction Types, by varying one parameter while fixing the rest.

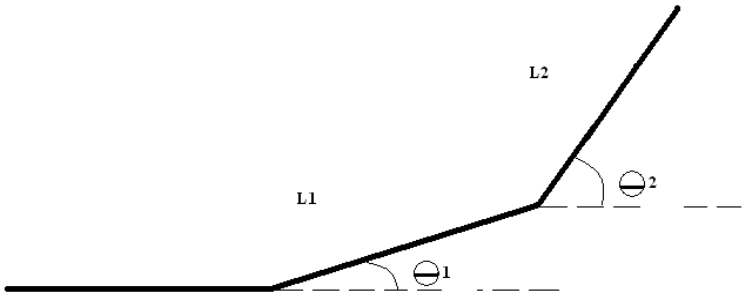

Figure 1 – Double wedge geometry concept.

To model flow structures for Type IV, V, and VI shock interactions, θ_1, M, and the length ratio L_1/L_2 are held constant. Following the work in reference [9], we fixed $L_1 = L_2 = 2$m (i.e. $L_1/L_2 = 1$), the first deflection angle at $\theta_1 = 15$ degrees, and the freestream Mach at M = 9 for all runs (Table 1). Hence, the only variable in our study is θ_2, the variation of which produces the various Types of shock interactions. The focus of our study is to validate our CFD results for the different Types of shock interactions.

Table 1 – Definition of the Types of shock interactions in terms of flow deflection angles.

Shock Type	1st flow deflection angle θ_1	2nd flow deflection angle θ_2	Freestream Mach number M
IV	15 degrees	50 degrees	9
V	15 degrees	45 degrees	9
VI	15 degrees	35 degrees	9

The boundary conditions in our model were set the follows:

- Inlet condition of Mach = 9
- Static pressure = 100,000 N/m^2
- Static temperature = 185 K
- Outlets were set at an extrapolated condition.

The initial conditions in our model were set are as follows:

- Static pressure = 1000 N/m^2
- Static temperature = 293 K.

All cases were ran for 10,000 cycles.

Grid Generation

Geometry creation and grid generation was done in CFD-GEOM. We modeled all our grids as structured. A close up of the grid surface deflection point of the geometry is shown in Figure 2. Grid condensation had to be applied and this greatly increased the computational run time as well as the effectiveness of our runs. To capture the flow separation, shock initiation, aerodynamic and thermal loads, and the boundary layer conditions, the grid was finer near the boundaries.

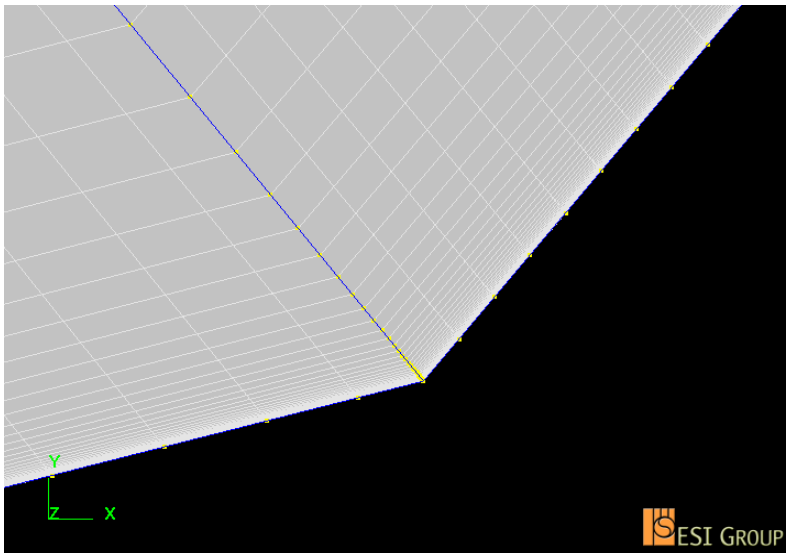

Figure 2 – Close up view of surface deflection point.

Table 2 shows the grid specifications for the different Types of shock interactions.

Table 2 – Summary of grid specifications

Interaction Type	Total # of cells	Total # of nodes	First spacing of the wall (m)	Stretching ratio	Converging factor
Type 4	13563	13775	1.5 E-06	1.25	1E-04
Type 5	11256	11475	2.0 E-06	1.25	1E-05
Type 6	18040	18315	1.5 E-06	1.25	1E-04

IV. Results

Type 4 Shock-Shock Interaction

The first Type of shock interaction that we explored was Type 4. As previously stated, the Mach number remains constant throughout all computations. Our CFD solutions are presented in Figures 3, 4, and 5. It may be seen, that when the flow passes the first wedge, the conditions are such that it generates a weak attached oblique shock wave, which reduces the Mach number from its freestream value of 9 to 5.70. This flow then interacts with the shockwave that forms at the second deflection angle. The figures show that a nearly normal shock is formed by the second wedge shockwave interaction. This newly formed shockwave curves slightly due to the intersection of the first shockwave. The characteristics of a Type 4 shock interaction are seen when the slip line is under conditions that do not let it reattach to the body. Under these conditions the flow generates a supersonic jet. A slip line means that the flow separates in two parts: a region above with subsonic flow and a region below with supersonic flow. Under these conditions the flow gives rise to a Type 4 interaction, which is also the interaction that gives rise to the highest thermal and pressure loads.

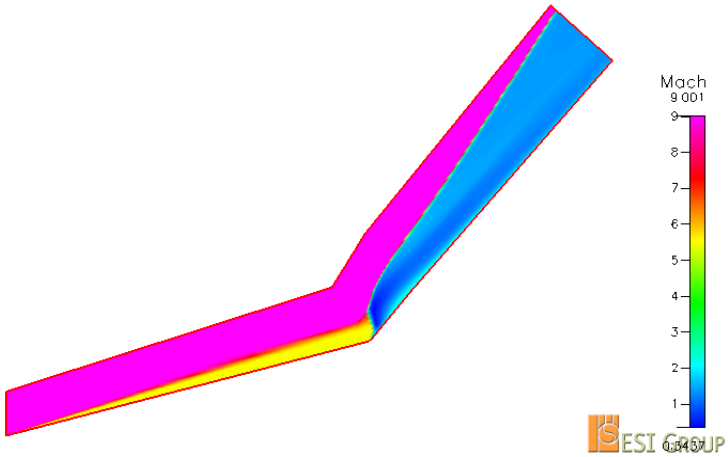

Figure 3 – Mach contour resulting in Type 4 shock interaction.

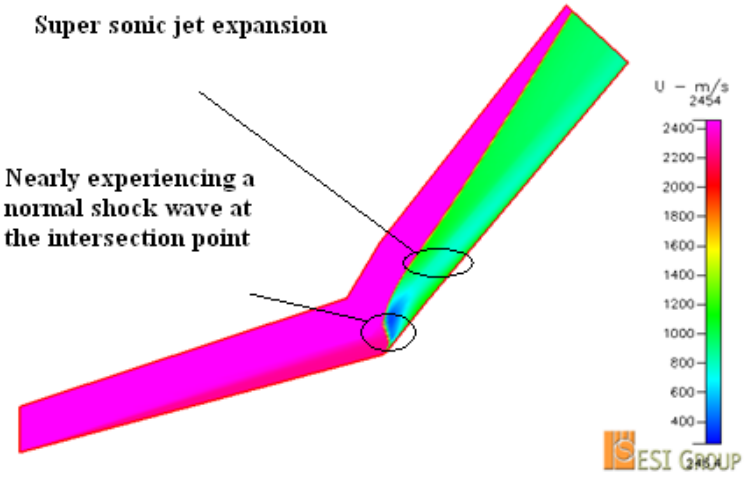

Figure 4 – Velocity solution in the x-direction.

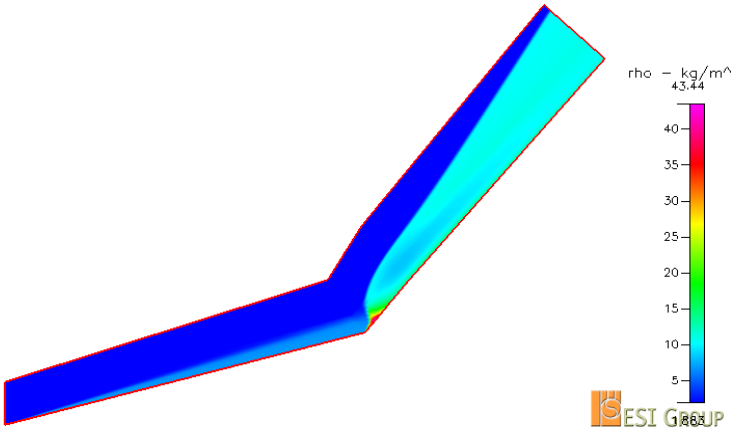

Figure 5 – Density distribution along the double wedge geometry at M=9, Type 4 interaction.

Benchmark

When comparing our result to Olejniczak[9], we verify that our results did not have such an area bounded by a sonic line encapsulating the subsonic region. Our results did however verify that a supersonic jet does form behind the nearly normal shockwave, just below the intersection point.

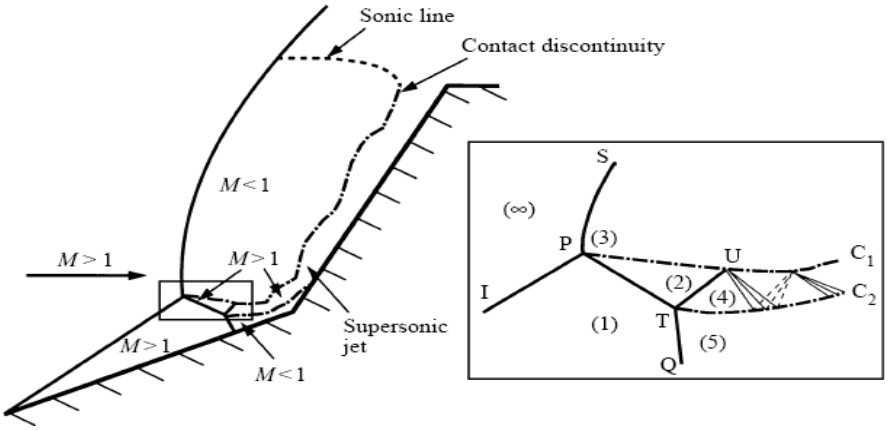

Figure 6 – Schematic of physical flow expected. (Olejniczak, Wright & Candler 1997)

Type 5 Shock-Shock Interaction

A Type 5 shock interaction was also modeled and the flow solution contours for the density and Mach number are shown in Figures 7 and 8 respectively. The shocks are categorized as weak and interact at the upper sonic line. A supersonic jet expanding in the flow field behind the interaction area of the second shock can also be seen in these figures. The density through the jet region is approximately 8 kg/m^3. This jet is embedded by a higher density above and below giving shape to the jet wake. The maximum density as was expected prior to our analysis is in the region where the intersection of the two initial shock waves occurs. The maximum density computed in this region is 30.78 kg/m^3. The Mach contour shown in Figure 8 verifies the weak oblique shock wave created at the first angle of the double wedge, along with the stronger shock wave at the second angle of the double wedge.

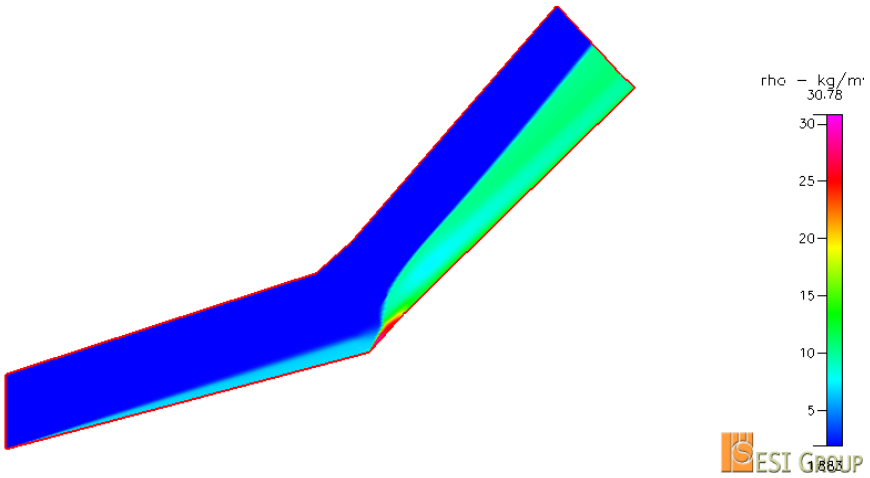

Figure 7 – Density distribution along the double wedge geometry at M=9, Type 5 interaction.

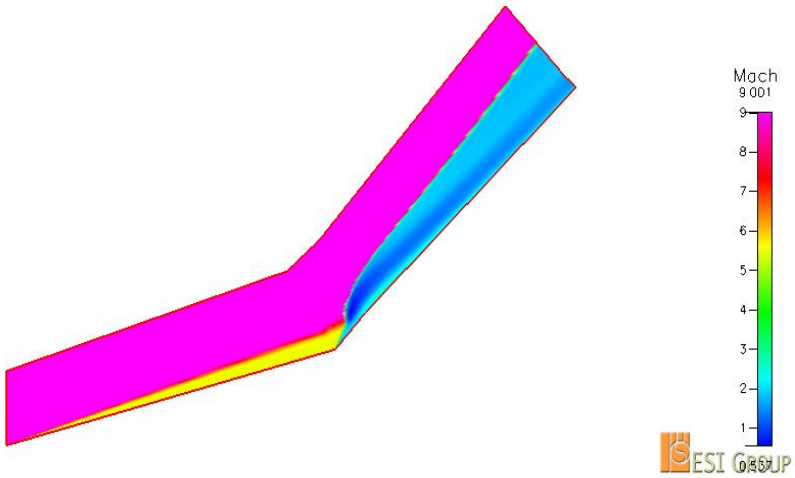

Figure 8 – Mach contour results for Type 5 shock interaction.

Benchmark

Our benchmark case for a Type 5 shock interaction is seen in Figure 9. For the flow to be classified as a Type 5 shock interaction, it must give rise to a sonic line, a supersonic jet, and a contact discontinuity. After running our cases, we obtained two of these three behaviors in our case models. A contact discontinuity is simply a path of mixing flow layers that gives a transition of density between two different flow masses, which is seen in Figure 7 and a supersonic jet which is evident in Figure 8. The sonic line is the only element that is not evident in our computational results.

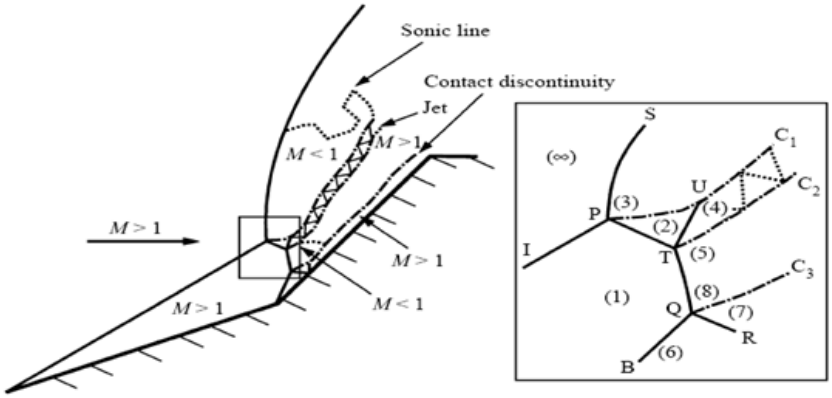

Figure 9 – Schematic for a Type 5 interaction[9].

Type 6 Shock-Shock Interaction

The final type of shock interaction that was characterized in our analysis was Type 6. As seen through Figure 12, when the two shockwaves interact far behind the surface deflection point, and a slip line as well as an expansion wave are present, we observe a typical Type 6 flow. The main difference between a Type 6 flow and a Type 4 or 5 flow is the absence of a jet. On the other hand, however there is an expansion wave in the Type 6 flow. The slip line in this case is more noticeable in the density contour solution shown in Figure 10.

The thin light blue line that is evident in Figure 10 is the slip line that is generated as a result of the interaction. This thin slip line seems to fade away due to the flow velocity increase. There is a noticeable flow velocity increase due to the fact that there is a small expansion wave in the flow that accelerates the outflow particles. The slip line disappears because there is no density gradient when the flow eventually reaches the same speeds on both sides.

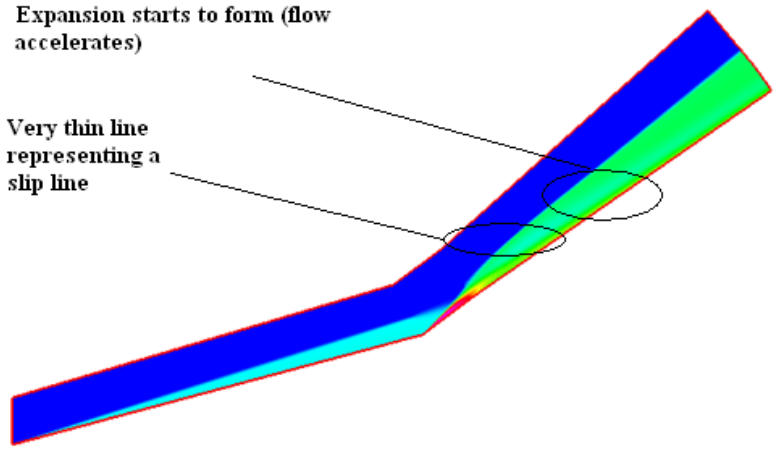

Figure 10 – Density distribution for a Type 6 shock interaction.

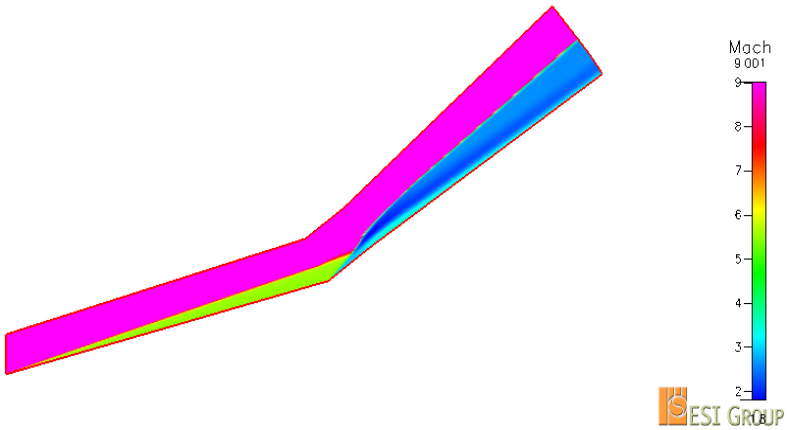

Figure 11 – Mach contour results for a Type 6 interaction.

Benchmark

Figure 12 illustrates the benchmark solution we use to compare our results. The Mach contours are very similar in both figures. The shock standoff distance is smaller for both shocks compared with the standoff distance for the Type 4 and 5 interactions. The interaction point along the second wedge surface is higher, compared to its location in the Type 4 and 5 interactions.

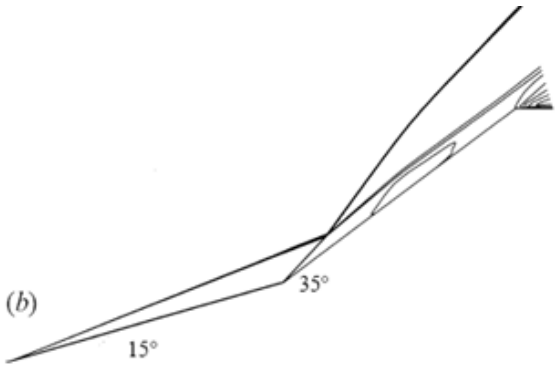

Figure 12 – Mach contour benchmark for a Type 6 shock interaction[9].

Heating Load Comparison

As mentioned earlier, one of the most critical effects of shock-shock interactions is the aerothermodynamic heating loads that different interaction types generate. Our results show that a Type 4 interaction causes the highest aerothermodynamic loads. The shockwave formed at the intersection curves slightly upward. The characteristics of a Type 4 shock-shock interaction are seen when the slip line is under conditions that it cannot reattach to the body. Under these conditions the flow generates a supersonic jet. The close proximity of this supersonic jet to the surface of the body is what causes the high temperatures observed in Figure 13. The maximum thermal load that we see in the Type 4 case is 3,270 K, which is higher than the corresponding thermal loads shown in Figures 14 and 15.

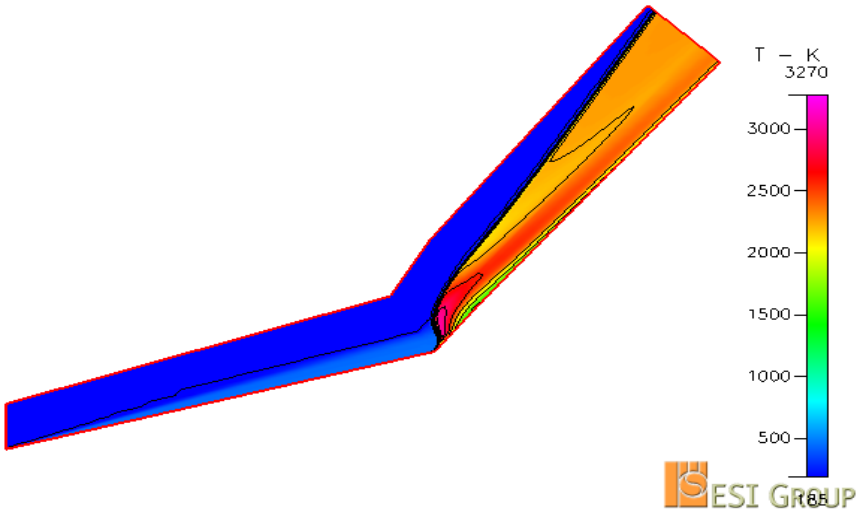

Figure 13 – Temperature contour distribution for Type 4, M=9 flow.

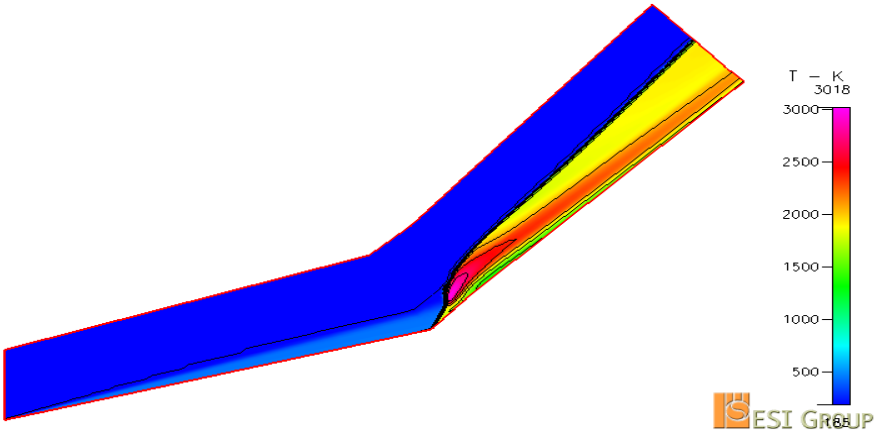

Figure 14 – Temperature contour distribution for Type 5, M=9 flow.

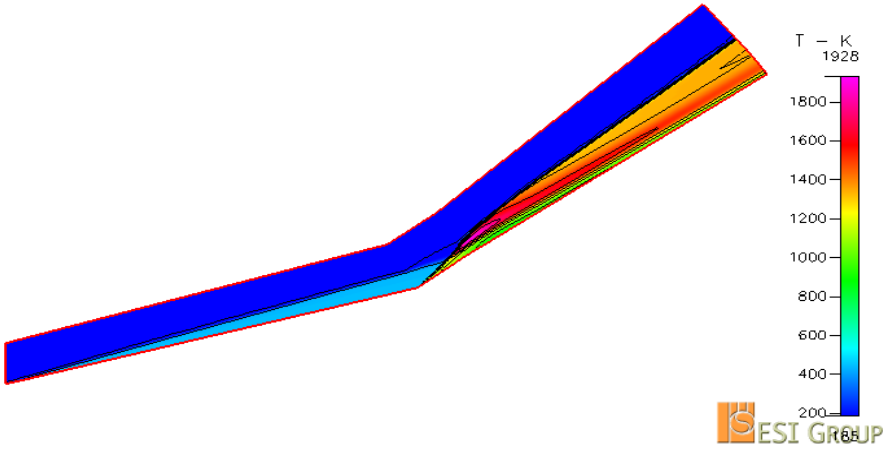

Figure 15 – Temperature contour distribution for Type 6, M=9 flow.

V. Conclusion

In this report we have successfully characterized the flow of Types 4, 5, and 6 shock interactions using CFD analysis and a double wedge geometry. The flow characteristics for various shock interaction Types were compared with results from previous investigations. In general our outflow results were similar to those in our benchmarks. We were able to capture the shockwaves generated at the intersection point, such as the nearly normal shocks seen in Types 4, and 5. Our results also captured the supersonic jet that is frequently present in the downstream flow and extends in most cases all along the near surface of the wedge. Finally, the slip line in our model was observed in a location similar to that shown in our benchmark papers.

Shock interactions have very important applications in the design of supersonic and hypersonic vehicles. The simple analysis presented in this paper is the first step in the creation of a model that will allow on one hand the prediction of aerodynamic and thermal loads for a given vehicle geometry and on the other the control of aerodynamic deceleration by varying this geometry.

Acknowledgments

Dr. Periklis Papadopoulos from San Jose State University for his guidance and support throughout this project.

References

[1] H.G. Hornung, M.L. Robinson, *Transition from regular to Mach reflection of shock waves. Part 2. The steady flow criterion*, J. Fluid Mech. 123 (155), 1982, 155–164.

[2] H.G. Hornung, H. Oertel, R.J. Sandeman, *Transition to Mach reflection of shock waves in steady and pseudosteady flow with and without relaxation*, J. Fluid Mech. 90 (541), 1979, 541–560.

[3] A. Chpoun, D. Passerel, H. Li, G. Ben-Dar, *Reconsideration of oblique shock wave reflection in steady flows. Part 1. Experimental investigations*, J. Fluid Mech. 301 (19), 1995, 19–35.

[4] B. Edney, *Anomalous heat transfer and pressure distributions on blunt bodies at hypersonic speeds in the presence of an impinging shock*, Aeronautical Research Institute of Sweden, Report 115, Stockholm, 1968.

[5] A.R. Wieting, M.S. Holden, *Experimental study of shock wave interference heating on a cylindrical leading edge*, AIAA J. 27 (11), 1989, 1557–1565.

[6] M.S. Holden, A.R. Wieting, J. Moselle, C.E. Glass, *Studies of aerothermal loads generated in regions of shock–shock interaction in hypersonic flow,* AIAA Paper 88-0477, January 1988.

[7] F.S. Billig, *Shock-wave shapes around spherical – and cylindrical – nosed bodies*, J. Spacecraft 4 (6), 1967.

[8] F. Grasso , C. Purpura , B. Chanetz , J. Délery ,*Type III and Type IV shock/shock interferences: theoretical and experimental aspects,* Aerospace Science and Technology vol. 7, pp. 93–106, 2003.

[9] J. Olejniczak, M.J. Wright, G.V. Candler, *Numerical study of inviscid shock interactions on double-wedge geometries,* J. Fluid Mechanics, vol. 352, p.1, Cambridge University Press, 1997.